JOURNAL OF SPACECRAFT AND ROCKETS
Vol. 31, No. 5, September–October 1994

An Improved Version of the Naval Surface Warfare Center Aeroprediction Code (AP93)

F. G. Moore,* T. Hymer,† and R. McInville†
Naval Surface Warfare Center, Dahlgren, Virginia 22448-5000

A new and improved version of the Naval Surface Warfare Center, Dahlgren Division aeroprediction code has been developed. The new code, AP93, contains new technology that allows planar aerodynamics ($\Phi = 0$ roll and in plus fin orientation) of axisymmetric solid-rocket-type weapons to be computed over the entire Mach-number range that weapons fly and for angles of attack (AOAs) up to 30 deg. New technology developed and contained in the AP93 includes a new engineering method to compute aeroheating information at high Mach number; extension of the second-order shock-expansion theory to incorporate real-gas effects, including several new pressure prediction techniques; an improved body-alone nonlinear normal-force method; new methods for computing the nonlinear aerodynamics of wing-alone, wing-body, and body-wing effects due to AOA, and wing-body effects due to control deflection; and a new base-drag database and improved empirical base-drag estimation technique. Comparisons of the new AP93 code with the AP81 and experimental data have been made on many different configurations. In general, the comparisons show the AP93 on average reduces the normal force and center-of-pressure errors of the AP81 code about in half and gives a slight improvement in axial force errors.

Nomenclature

A_{ref} = reference area (maximum cross-sectional area of body if a body is present or planform area of wing if wing alone), ft^2
A_w = planform area of wing in crossflow plane, ft^2
AR = aspect ratio = b^2/A_W
b = wingspan (not including body), ft
C_A = axial-force coefficient
C_M = pitching-moment coefficient (based on reference area and body diameter if body present, or mean aerodynamic chord if wing alone)
C_N = normal-force coefficient
C_{NT} = normal-force coefficient of tail
$C_{NT(V)}$ = negative normal-force coefficient component on tail due to wing or canard shed vortex
$C_{N\alpha}$ = normal-force coefficient derivative
d_{ref} = reference body diameter, ft
F = dimensionless empirical factor used in tail normal-force coefficient term to approximate nonlinear effects due to a control deflection of a forward control surface
f_w, f_t = lateral location of wing or tail vortex (measured in feet from body centerline)
i = tail interference factor
$K_{B(W)}$ = ratio of additional body normal-force coefficient due to presence of wing to wing-alone normal-force coefficient at $\delta = 0$
$K_{W(B)}$ = ratio of normal-force coefficient of wing in presence of body to that of wing alone at $\delta = 0$
$k_{B(W)}$ = ratio of additional body normal-force coefficient due to presence of wing at a control deflection to that of the wing alone
$k_{W(B)}$ = ratio of wing normal-force coefficient in presence of body due to a control deflection to that of wing alone
$[k_{W(B)}]_{\text{SB}}$ = value of $k_{W(B)}$ calculated by slender-body theory
M_∞ = freestream Mach number = V/a
r_w, r_t = radius of body at wing or tail location
r/s = ratio of body radius to wing or tail semispan plus the body radius
x_{cp} = center of pressure (in feet or calibers from some reference point that can be specified)
α = angle of attack, deg
α_w, α_T = local angle of attack of wing or tail ($\alpha + \delta_W$ or $\alpha + \delta_T$, respectively), deg
δ_w, δ_T = deflection of wing or tail surfaces (plus leading edge up), deg
λ = taper ratio of a lifting surface = c_t/c_r
Λ = leading edge sweep angle of wing or tail (degrees)

Introduction and Background

THE purpose of this paper is threefold. First, the paper summarizes the theoretical and empirical methods that are included in the new nonlinear missile aeroprediction code (AP93). It also shows the methods that will be retained from the former aeroprediction code (AP81). Secondly, results of calculations for static aerodynamics using the AP93 and AP81 are given to provide insight into the improvements attained by the new technology added to AP93. Finally, new technology for nonlinear wing-body interference for control deflections and for reductions in wing nonlinear lift in transonic flow, not previously presented in the external literature, are introduced, and results are given.

The four previous versions of the Naval Surface Warfare Center, Dahlgren Division (NSWCDD) aeroprediction code (APC) were documented[1–7] and transmitted to users in 1972, 1974, 1977, and 1981. Each of these versions attempted to meet the requirements as seen by the tactical weapons community. The first version[1] was for general-shaped bodies alone. It was the first such code known that combined a good mix of accuracy in aerodynamic computations with ease of use and economy of computational time. It is believed that this mix led to the code's initial popularity and requests for additional capability. In 1974,[2,3] the code was extended to allow up to two sets of lifting surfaces in the computational process. In 1977,[4,5] dynamic aerodynamic derivatives were added to the code's capability. Finally, the last version of the code[6,7] extended the Mach-number range up to 8 and added high-AOA capability for a narrow range of configurations.

Over the past 10 years, the AP81 has been used to compute aerodynamics on configurations at conditions where the accuracy is not good. This includes AOAs greater than about 15 deg on missiles with two sets of lifting surfaces and at Mach numbers greater than

Received Aug. 24, 1993; revision received Feb. 17, 1994; accepted for publication Feb. 23, 1994.

*Senior Aerodynamicist in Weapons Systems Department, Dahlgren Division. Associate Fellow AIAA.
†Aerospace Engineer, Aeromechanics Branch, Dahlgren Division.

8, where real-gas effects become important in the aerothermal environment. Furthermore, the base-drag estimation, while including AOA and first-order fin effects, needed additional wind-tunnel data for more accurate computations. As a result of these known shortcomings, a desire to still use the APC, and the fact that there was no accurate engineering code available to accomplish the objectives of AOA, Mach-number, and base-drag prediction capability, an effort was begun in 1990 to extend the APC to meet these requirements.

The extension of the code to hypersonic Mach numbers, including real-gas effects, was completed and documented.[8,9] In the development of this new technology, three new pressure prediction methods were derived, along with a method for accurately estimating inviscid surface temperatures. The inviscid surface temperatures were then used to develop an engineering method for boundary-layer heating.[10] The new method thus provides engineering estimates of adiabatic wall-temperature and heat-transfer coefficients for configurations flying at hypersonic Mach numbers and at AOA.

New methods for nonlinear wing-alone, wing-body, and body-wing normal forces were recently developed.[11,12] In addition, an improved body-alone, nonlinear normal-force prediction capability was developed. Improved center-of-pressure estimates were added that gave improved pitching moments. The code's AOA range is now 0 to 30 deg in the planar or ($\Phi = 0$) roll position.

Wind-tunnel tests were conducted to measure base pressure as a function of Mach number, AOA, fin thickness, fin location, and fin deflection. Using these data, an improved empirical base-drag prediction methodology has been developed.[13,14]

A new nonlinear method for wing-body interference, due to control deflection, has recently been developed. This new technology, along with empirical improvements for nonlinear aerodynamic estimates in the transonic flow regime, is also given in this paper.

Analysis and Methods Summary

The introduction listed three main purposes for this paper. It is most convenient to discuss the third purpose first. There are two primary new semiempirical technologies not presented previously that need to be discussed. These include a nonlinear method for the wing-body normal force due to control deflection and an empirical correction for shock-wave losses on the wing normal force in the transonic speed region.

Nonlinear Wing-Body Interference Due to Control Deflection

The total configuration normal-force coefficient at a given AOA, control deflection, and Mach number is[15]

$$C_N = C_{NB} + [(K_{W(B)} + K_{B(W)})\alpha + (k_{W(B)} + k_{B(W)})\delta_W](C_{N\alpha})_W + [(K_{T(B)} + K_{B(T)})\alpha + (k_{T(B)} + k_{B(T)})\delta_T](C_{N\alpha})_T + C_{NT(V)} \quad (1)$$

The first term in Eq. (1) is the normal force of the body alone, including the linear and nonlinear components; the second term is the contribution of the wing (or canard), including interference effects and control deflection; the third term is the contribution of the tail, including interference effects and control deflection; and the last term is the negative downwash effect on the tail due to wing shed or body shed vortices. The capital K's represent the interference of the configuration with respect to AOA, and the lowercase k's represent the interference with respect to control deflection. The subscripts $W(B)$ and $T(B)$ represent the change (or interference effect) of the wing and tail in the presence of the body, whereas the subscripts $B(W)$ and $B(T)$ indicate the additional lift (or interference effect) on the body due to the presence of wings or tails.

References 1–7 used a combination of first-order theory [16–18] and Allen-Perkins viscous crossflow[19] for the body-alone term of Eq. (1). Slender-body or linearized theory was used for the remaining terms of Eq. (1). Improvements in the body-alone contribution to Eq. (1), along with nonlinear contributions to the wing-alone, wing-body, and body-wing forces, were derived and reported in Refs. 11 and 12. Initial plans, as indicated in Refs. 11 and 12, were to use slender-body theory for the wing-body and body-wing contributions due to control deflection (lowercase k's). However, in implementing the nonlinear methodology of Refs. 11 and 12 with control deflection, it was found that a nonlinear contribution was needed for those terms as well. The fundamental problem has to do with the fact that slender-body theory is independent of Mach number, AOA, and control deflection. It is a function of r/s only. What actually happens is that at low Mach number, slender-body theory gives slightly low values for $k_{W(B)}$ at low AOA. When the total AOA to the wing ($|\alpha+\delta|$) is increased above about 25 deg, the value of $k_{W(B)}$ starts decreasing until about 55 deg, where it is zero. In other words, the slope of the wing lift curve no longer increases substantially with AOA, and the controls lose effectiveness. On the other hand, at high supersonic Mach numbers, exactly the opposite effects occur. At low AOA, slender-body theory gives values of $k_{W(B)}$ higher than data suggest, whereas at higher AOA, the actual values of $k_{W(B)}$ increase due to compressibility effects. The controls are therefore more responsive as AOA increases.

In addition, it was found that the vortex lift on the tail, due to wing or canard shed vortices [last term of Eq. (1)], also required an empirical correction when the forward controls were deflected. A summary of this new nonlinear methodology for control deflections will be given. For details, refer to Ref. 20.

Using Refs. 21–23 for low Mach number, a semiempirical nonlinear model for $k_{W(B)}$ and the parameter F was derived from numerical experiments. The mathematical model for $k_{W(B)}$ is based on slender-body theory similar to $K_{W(B)}$ and $K_{B(W)}$ and modified for AOA or control deflection. In general, it was found that

$$k_{W(B)} = C_1(M)[k_{W(B)}]_{SB} + C_2(|\alpha_W|, M_\infty)$$
$$F = C_3(M, |\alpha_W|) \quad (2)$$

More specifically, $k_{W(B)}$, C_1, C_2, and F are defined in Fig. 1 for Mach numbers where data are available. For Mach numbers less than 0.8 and greater than 4.6, the equations derived for those conditions have been used. The current method for using the empirical estimate for $k_{W(B)}$ in Fig. 1 is to interpolate linearly between Mach numbers for a given set of values of α, δ, and M_∞.

The parameter F of Eq. (2) is used only in the last term of Eq. (1), as shown in

$$C_{NT(V)} = \frac{(C_{N\alpha})_W (C_{N\alpha})_T i (S_T - r_T) A_W}{2\pi (\mathrm{AR})_T (f_W - r_W) A_{\mathrm{ref}}} \times [K_{W(B)} \sin\alpha + F k_{W(B)} \sin\delta_W] \quad (3)$$

This equation has the same form as in Ref. 15, except all the aerodynamic parameters are nonlinear in AOA, as developed in Ref. 20, and the factor F has been inserted.

In addition to the nonlinear $k_{W(B)}$ model of Eqs. (2) and (3), where the constants are defined in Fig. 1, it was found necessary to provide an upper limit on values computed by Eq. (3). This upper limit primarily concerns cases that have large values of A_W/A_{ref}, the factor in Eq. (3) that converts the loss of lift on the tail to the body cross-section area. In some cases, it was found that values of $C_{NT(V)}$ actually exceeded the tail lift. In comparing results from Eq. (3) with experimental data on cases where the wings are large, an upper bound was defined, as a percentage of the tail lift; it is of Mach number and AOA. Its values are given by

$$M_\infty \le 1.0: \quad [C_{NT(V)}]_{\max} = -(0.90 - 0.0183\alpha) C_{NT} \quad (4a)$$

$$M_\infty = 1.6: \quad [C_{NT(V)}]_{\max} = -(0.85 - 0.0200\alpha) C_{NT} \quad (4b)$$

$$M_\infty \ge 4.5: \quad [C_{NT(V)}]_{\max} = -(0.55 - 0.010\alpha) C_{NT} \quad (4c)$$

Linear interpolation for maximum values of $C_{NT(V)}$ is used for Mach numbers between those of Eq. (4).

In developing this nonlinear interference methodology for control deflection, it should be pointed out that the initial approach was to use the large NASA–Tri Service database to try and separate out the effects due to control deflection from other parameters. However, due to the small size of many fins compared to the body planform size, this proved to be impractical. It should also be pointed out that the parameters C_1, C_2, and F were derived without any explicit

$$\underline{M \leq .8}$$

$$\text{If } |\alpha_w| \leq 24.0 \rightarrow k_{w(B)} = 1.4[k_{w(B)}]_{SB}$$
$$\text{If } |\alpha_w| > 24.0 \rightarrow k_{w(B)} = 1.4\,[.000794\,|\alpha_w|^2 - .0933\,|\alpha_w| + 2.71]$$

$$\underline{M = 1.1}$$

$$\text{If } |\alpha_w| \leq 15.0 \rightarrow k_{w(B)} = 1.3[k_{w(B)}]_{SBT}$$
$$\text{If } |\alpha_w| > 15.0 \rightarrow k_{w(B)} = 1.3\,[.00087\,|\alpha_w|^2 - .0825\,|\alpha_w| + 2.71]$$

$$\underline{M = 1.5}$$

$$\text{If } |\alpha_w| \leq 10.0 \rightarrow k_{w(B)} = .9[k_{w(B)}]_{SB}$$
$$\text{If } |\alpha_w| > 10.0 \rightarrow k_{w(B)} = .9[k_{w(B)}]_{SB} - .015[|\alpha_w| - 10.0]$$
$$\text{If } |\alpha_w| \leq 20.0 \rightarrow F = .8$$
$$\text{If } |\alpha_w| > 20.0 \rightarrow F = .8 + .10[|\alpha_w| - 20.0]$$

$$\underline{M = 2.0}$$

$$\text{If } |\alpha_w| \leq 10.0 \rightarrow k_{w(B)} = .9[k_{w(B)}]_{SB}$$
$$\text{If } |\alpha_w| > 10.0 \rightarrow k_{w(B)} = .9[k_{w(B)}]_{SB} - .005[|\alpha_w| - 10.0]$$
$$\text{If } |\alpha_w| \leq 20.0 \rightarrow F = .8$$
$$\text{If } |\alpha_w| > 20.0 \rightarrow F = .8 + .17[|\alpha_w| - 20.0]$$

$$\underline{M = 2.3}$$

$$\text{If } |\alpha_w| \leq 20.0 \rightarrow k_{w(B)} = .95[k_{w(B)}]_{SB}$$
$$\text{If } |\alpha_w| > 20.0 \rightarrow k_{w(B)} = .95[k_{w(B)}]_{SB} - .005[|\alpha_w| - 20.0]$$
$$\text{If } |\alpha_w| \leq 30.0 \rightarrow F = .9$$
$$\text{If } |\alpha_w| > 30.0 \rightarrow F = .9 + .15[|\alpha_w| - 30.0]$$

$$\underline{M = 2.87}$$

$$\text{If } |\alpha_w| \leq 20.0 \rightarrow k_{w(B)} = .9[k_{w(B)}]_{SB}$$
$$\text{If } |\alpha_w| > 20.0 \rightarrow k_{w(B)} = .9[k_{w(B)}]_{SB} - .005[|\alpha_w| - 20.0]$$
$$\text{If } |\alpha_w| \leq 30.0 \rightarrow F = .9$$
$$\text{If } |\alpha_w| > 30.0 \rightarrow F = .9 + .17[|\alpha_w| - 30.0]$$

$$\underline{M = 3.95}$$

$$k_{w(B)} = .9[k_{w(B)}]_{SB}$$
$$\text{If } |\alpha_w| \leq 40.0 \rightarrow F = 0.8$$
$$\text{If } |\alpha_w| > 40.0 \rightarrow F = 0.8 + .4[|\alpha_w| - 40.0]$$

$$\underline{M \geq 4.6}$$

$$\text{If } |\alpha_w| \leq 20.0 \rightarrow k_{w(B)} = 0.75[k_{w(B)}]_{SB}$$
$$\text{If } |\alpha_w| > 20.0 \rightarrow k_{w(B)} = 0.75[k_{w(B)}]_{SB} + .01[|\alpha_w| - 20.0]$$
$$\text{If } |\alpha_w| \leq 35.0 \rightarrow F = .9$$
$$\text{If } |\alpha_w| > 35.0 \rightarrow F = .9 + .3[|\alpha_w| - 35.0]$$

where $\alpha_w = \alpha + \delta$

Fig. 1 Nonlinear wing-body interference model due to control deflection.

body shed vortices included in the AP93. This means that if one is interested in using this technology in a code that already explicitly predicts body shed vortex effects, these effects could be duplicated. In other words, the parameters C_1, C_2, and F are empirical corrections to slender-body theory that allow for the fact that slender-body theory is independent of Mach number, AOA, and control deflection, as well as the fact that there are no explicit body shed vortices in the AP93.

Loss of Nonlinear Normal Force in Transonic Flow

A second problem associated with the new nonlinear methodology presented in Refs. 11 and 12 was encountered in the transonic flow regime ($0.5 \leq M_\infty \leq 2.0$). This problem had to do with the apparent loss of nonlinear lift at AOAs greater than about 10 to 12 deg. It is suspected that as the AOA increases in the transonic region, shock waves form on the upper part of the fins, causing the flow to separate; hence, a loss of lift. It is also suspected that a loss of interference lift between the wing and body occurs for the same reason. Only experimental data or detailed numerical codes could verify this hypothesis. The bottom line is that, for bodies with wings, a loss of lift occurs in the vicinity of the wing at moderate AOAs in the transonic speed regime, causing the pitching moments and center of pressure to change correspondingly.

To address this nonlinear lift loss, several configurations were analyzed using the recent nonlinear methodology.[11,12] It was found that when the aspect ratio was moderate to high (AR $\geq$ 1.4), this methodology did a reasonable job in estimating the lift loss. The reason was the wing-alone lift curve was second-order and concave down. On the other hand, when AR was low (< 1.4), the wing-alone lift curve was second-order and concave upward. The real wing-lift curves for these conditions of transonic flow and low AR were of third order. For low α the curves were concave up, and for moderate

Table 1 Loss of wing nonlinear normal force due to shock-wave effects in transonic flow

	ΔC_N								
M_∞	$1\alpha + \delta 1 = 0$	5	10	15	20	25	30	35	40 deg
≤ 0.4	0.000	0.000	0.000	0.000	0.000	0.000	0.000	0.000	0.000
0.6	0.000	0.000	0.000	0.000	−0.022	−0.206	−0.689	−0.950	−1.300
0.8	0.000	0.000	0.000	0.000	−0.053	−0.220	−0.710	−1.010	−1.400
1.2	0.000	0.000	−0.009	−0.029	−0.165	−0.417	−0.763	−1.070	−1.500
1.5	0.000	0.000	−0.065	−0.111	−0.156	−0.444	−0.700	−1.070	−1.500
2.0	0.000	0.000	−0.008	−0.038	−0.150	−0.114	−0.095	−0.070	−0.050
≥ 2.5	0.000	0.000	0.000	0.000	0.000	0.000	0.000	0.000	0.000

Component/ Mach Number Region	Subsonic $M_\infty < 0.8$	Transonic $0.8 \leq M_\infty < 1.2$	Low Supersonic $1.2 \leq M_\infty \leq 2.4$	High Supersonic $2.4 < M_\infty \leq 6.0$	Hypersonic $M_\infty > 6.0$
Nose Wave Drag	–	Semiempirical based on Euler Solutions	Second-Order Van Dyke plus MNT	SOSET plus IMNT	SOSET plus IMNT Modified for Real Gases
Boattail or Flare Wave Drag	–	Wu and Aoyoma	Second-Order Van Dyke	SOSET	SOSET for Real Gases
Skin Friction Drag	Van Driest II				
Base Drag	Improved Empirical Method				
Aeroheating Information	–	–	–	–	SOSET plus IMNT for Real Gases
Inviscid Lift and Pitching Moment	Empirical	Semiempirical based on Euler Solutions	Tsien First-Order Crossflow	SOSET	SOSET for Real Gases
Viscous Lift and Pitch Moment	Improved Allen and Perkins Crossflow				

Fig. 2a AP93 methods for body-alone aerodynamics.

Component/ Mach Number Region	Subsonic $M_\infty < 0.8$	Transonic $0.8 \leq M_\infty < 1.2$	Low Supersonic $1.2 \leq M_\infty \leq 2.4$	High Supersonic $2.4 < M_\infty \leq 6.0$	Hypersonic $M_\infty > 6.0$
Wave Drag	–	Empirical	Linear Theory plus MNT	Shock Expansion (SE) plus MNT Along Strips	SE plus MNT for Real Gases Along Strips
Skin Friction Drag	Van Driest II				
Trailing Edge Separation Drag	Empirical				
Body Base Pressure Caused by Tail Fins	Improved Empirical				
Inviscid Lift and Pitching Moment • Linear • Nonlinear	Lifting Surface Theory Empirical	Empirical Empirical	3DTWT Empirical	3DTWT or SE Empirical	3DTWT or SE Empirical
Wing-Body, Body-Wing Interference • Linear • Nonlinear	Slender-Body Theory or Linear Theory Modified for Short Afterbodies Empirical				
Wing-Body Interference due to δ • Linear • Nonlinear	Slender-Body Theory Empirical				
Wing Tail Interference	Line Vortex Theory with Empirical Modifications for $k_{W(B)}$ Term and Nonlinearities				
Aeroheating	None Present				SE plus MNT for Real Gases

Fig. 2b AP93 methods for wing-alone and interference aerodynamics.

Component/Mach Number Region	Subsonic $M_\infty < 0.8$	Transonic $0.8 \leq M_\infty < 1.2$	Low Supersonic $1.2 \leq M_\infty \leq 2.4$	High Supersonic $2.4 < M_\infty \leq 6.0$	Hypersonic $M_\infty > 6.0$
Body Alone	Empirical				
Wing and Interference Roll Damping Moment	Lifting Surface Theory	Empirical	Linear Thin Wing Theory	Linear Thin Wing Theory or Strip Theory	
Wing Magnus Moment	Assumed Zero				
Wing and Interference Pitch Damping Moment	Lifing Surface Theory	Empirical	Linear Thin Wing Theory	Linear Thin Wing Theory or Strip Theory	

Fig. 2c AP93 methods for dynamic derivatives.

to high α they were concave down. As a result of this analysis, a table of ΔC_N was estimated (Table 1), based on a configuration of A_W/A_{ref} of about 1, as a function of M_∞ and α. This table has been implemented into the methodology of Refs. 11 and 12 by subtracting it from the $C_{NB(W)}$ term after multiplying it by the actual value of A_W/A_{ref} for the planform of interest. The pitching moment and center of pressure are then automatically adjusted in the APC.

Other Methods in AP93

New technology developed for the AP93 version APC and previously published includes

1) Extension of the second-order shock-expansion method to include real-gas effects.[8,9]

2) Incorporation of aeroheating methodology.[10]

3) New nonlinear lift methods for wing-alone, wing-body, and body-wing lift.[11,12]

4) Improved body-alone nonlinear lift method.[11,12]

5) Improved base-drag prediction technique.[13,14]

The essence of the new capability added is to give the AP93 code the ability to estimate aerodynamics at any Mach number of interest to weapon designers, including the ability to predict heat transfer at hypersonic Mach numbers, where heating becomes of utmost concern. In addition, the new nonlinear AOA methodology on average reduces the normal-force and center-of-pressure errors in the AP93 by about a factor of 2 in comparison with the AP81. The worst-case errors have been reduced even more. Finally, base-drag estimates can now be made with the variables base diameter, fin thickness, fin location, fin control deflection, and body AOA included.

Methods retained from AP81 in the AP93 code include most of the drag prediction methodology, as well as the linear lift techniques for wing-body and interference effects (see Refs. 1–7 for the theoretical details of these methods). These methods have given reasonably good estimates of planar aerodynamics for small AOAs. For some configurations, reasonable estimates of aerodynamics can be obtained up to 20-deg AOA. However, the AP93 nonlinear methods give significant improvements over the AP81 version for low- or high-aspect-ratio configurations at moderate to high AOA or at low or high Mach number. If the configuration has an aspect ratio of about 1 (where the nonlinearities are smallest), the AP81 code gives good results up to moderate AOAs. In some cases, the AP81 code actually gives slightly better results than the AP93 code.

A summary of the methods used for the body-alone, wing-alone, and interference effects and for dynamic derivatives is given in Fig. 2. While the number of new methods has been increased in the AP93 code from the AP81 code, some fairly large, but duplicative, subroutines have been removed. As a result, the code size (about 16 k lines), computer storage (132 k words), and computational time (less than 1 s on a CDC 990) per case (which is one Mach number and one AOA) of the two versions are about the same.

In examining Fig. 2, it is seen that the low-AOA methods are primarily theoretically based, with mostly second-order techniques used for the axial force, and first-order linear approaches used in the lift direction. On the other hand, most of the nonlinear methods are primarily empirical in nature.

Users of the code are once again reminded of the nonlinear aerodynamical effects not included in the code. These include out-of-plane and cross-coupling aerodynamic effects along with internal shock interactions. No explicit body-shed-vortex methodology is included; however, it is believed this effect is modeled approximately by being inherent in all the databases used.

Results and Discussion

Several configurations where wind-tunnel results are available have been chosen for comparison with the new AP93 code. In addition, results of the AP81 code are shown in order to illustrate the range of aeroprediction accuracy improvement afforded by the new code.

The first case considered is a body-tail configuration, shown in Fig. 3a, with data taken from Ref. 24. The case shown is for Mach 1.6 and control deflection of +10 deg. This figure illustrates the new nonlinear control-deflection methodology of Fig. 1 and the transonic

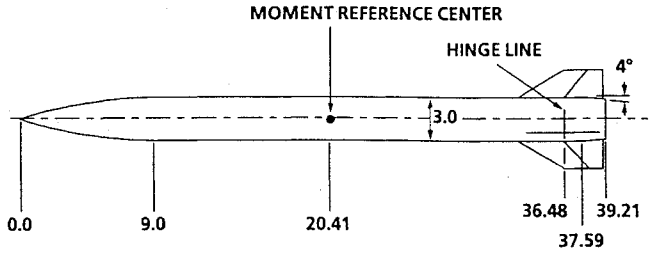

a) Geometry

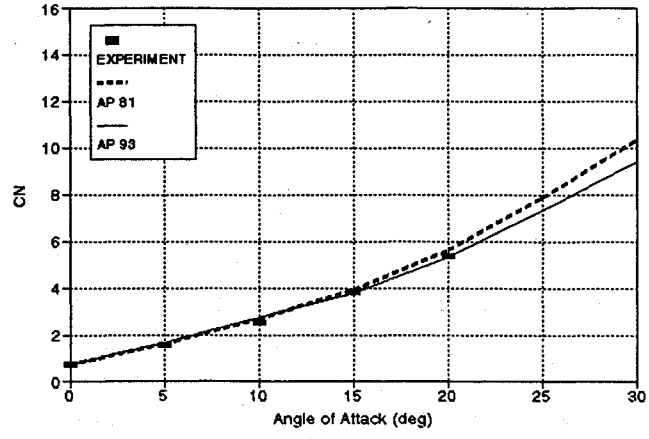

b) Normal force coefficient

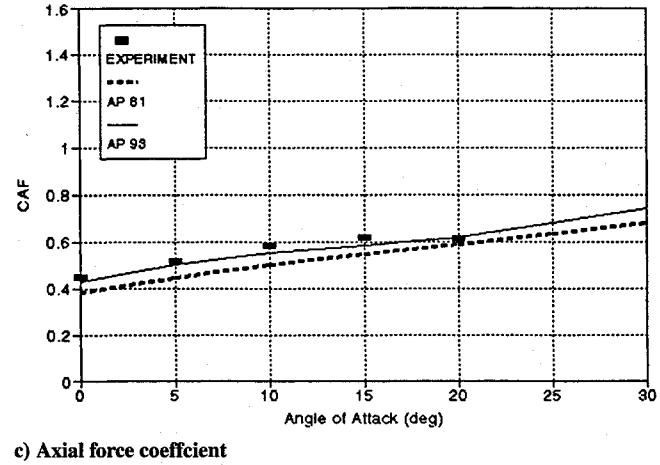

c) Axial force coeffcient

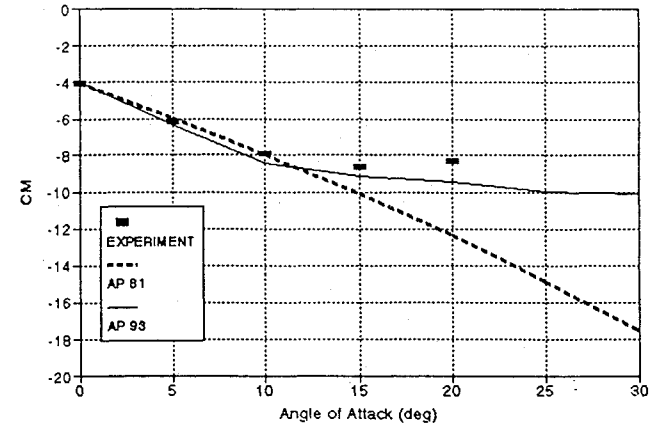

d) Pitching-moment coefficient

Fig. 3 Body-tail configuration comparisons at $M_\infty = 1.6, \delta = 10$ deg.

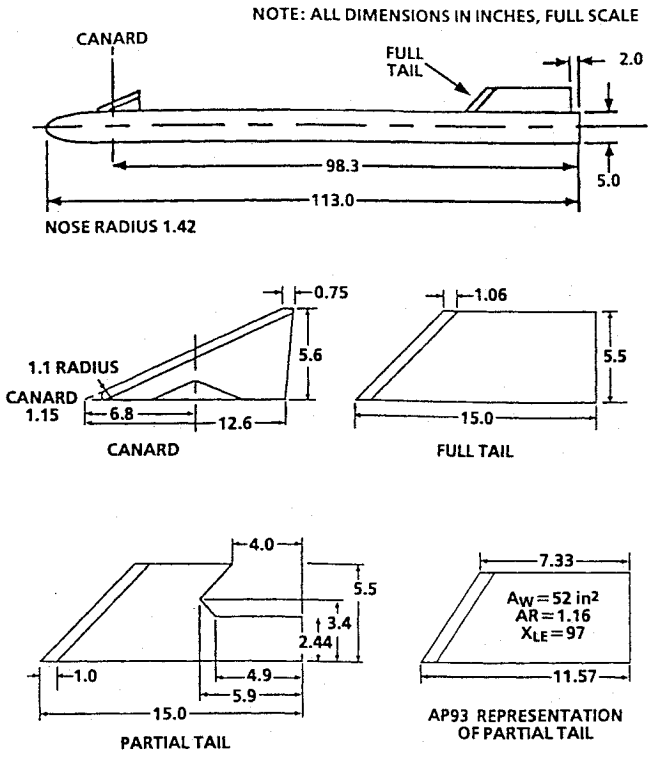

a) Geometry showing full-tail, partial-tail, and AP93 representation of partial-tail (dimensions in inches).

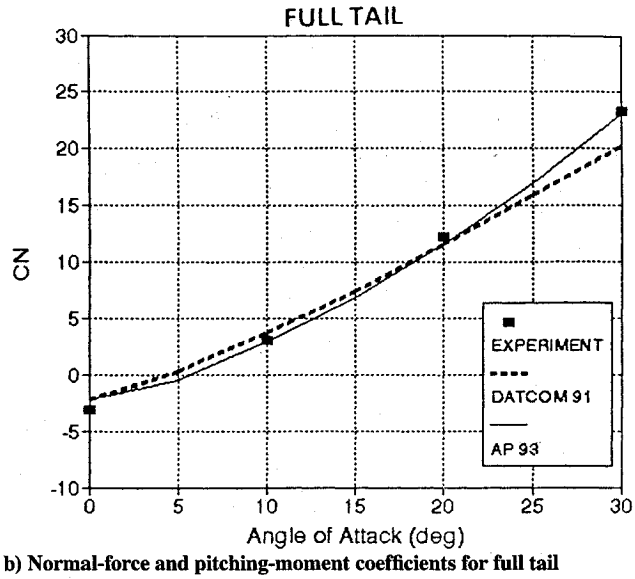

b) Normal-force and pitching-moment coefficients for full tail

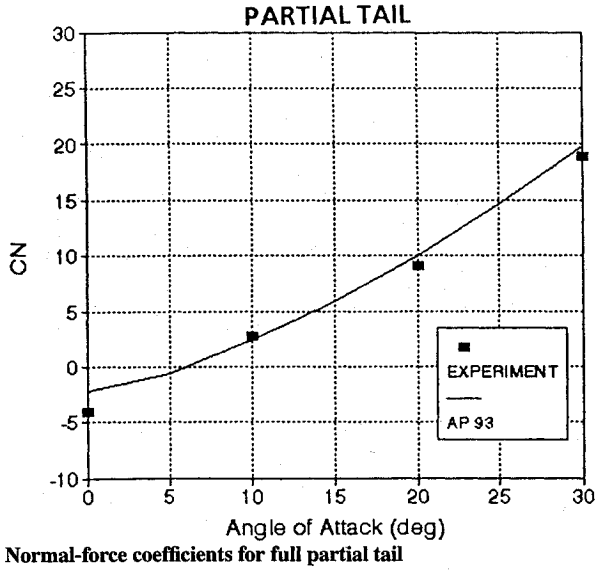

c) Normal-force coefficients for full partial tail

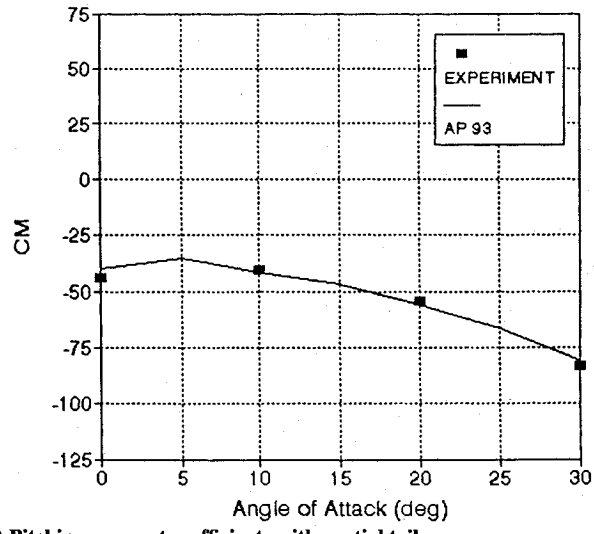

d) Pitching-moment coefficients with partial tail

Fig. 4 Canard control missile[23] configuration comparisons for $M_\infty = 0.2$, $\delta = -20$ deg.

nonlinear normal-force loss in the tail region due to shock-wave formation. The AP93 code gives agreement with forebody axial- and normal-force coefficient data that is slightly superior to the AP81 and experiment. However, significant improvement in pitching moment is attained, primarily due to the Table 1 data. It should also be pointed out that a base-pressure correction term was available in Ref. 24, but it apparently was taken inside the model cavity rather than at the base. These values differed substantially from a base drag, and therefore only the forebody axial force was shown.

A second case is based on data taken by Smith et al.[23] on a canard-controlled missile configuration. The data were taken on both a full- and a partial-tail configuration (see Fig. 4a). The partial-tail configuration had to be modeled for use in the AP93 as shown in Fig. 4a. In this modeling, the tail significant parameters are held constant. These include area, aspect ratio, span, and distance to centroid of area. Also, taper ratio and leading-edge sweep are approximately matched. The chord is allowed to vary so the above constraints can be met. Only $M_\infty = 0.2$ data were available, and results are shown in Fig. 4b for the full-tail case and Figs. 4c and 4d for the partial tail. Results are shown only for normal-force and pitching-moment coefficients at $\delta_c = -20$ deg. In this case, Missile DATCOM[25] computations were available in Ref. 23 for the full-tail configuration, and they are shown as well. Note the AP93 shows improved predictions over Missile DATCOM for both C_N and C_M at most AOAs. Of particular note is the improvement in pitching moment. The center of pressure at $\alpha = 30$ deg predicted by data, AP93, and Missile DATCOM are 5.43, 5.96, and 3.75 calibers, respectively. Because the total body length is 22.6 calibers, the center-of-pressure errors in percent of body length at this condition for the AP93 and Missile DATCOM are 2.3 and −7.4% respectively.

A third case considered is the air-to-air missile configuration shown in Fig. 5a. Wind-tunnel data[21,22] are available at Mach numbers from 1.5 to 4.6 and at various wing-control deflections. Only

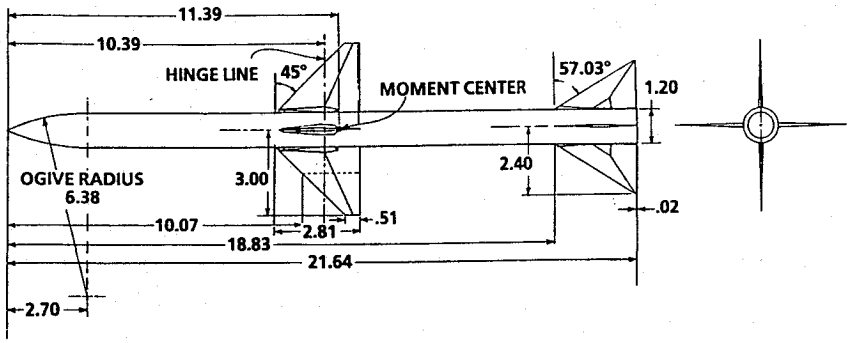

a) Geometry

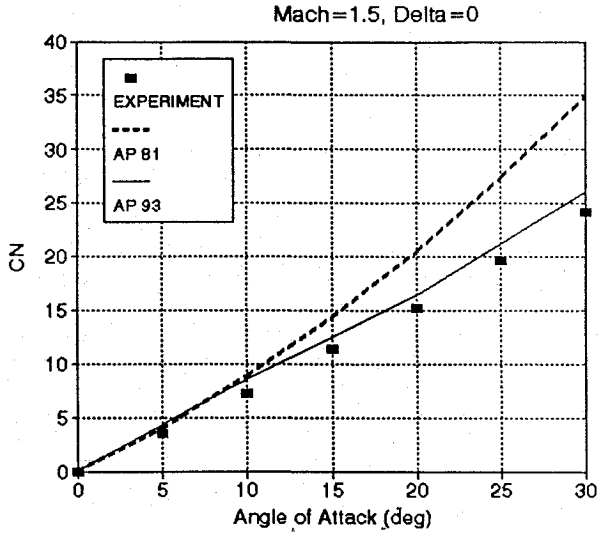

b) Normal force coefficient at $M_\infty = 1.5$

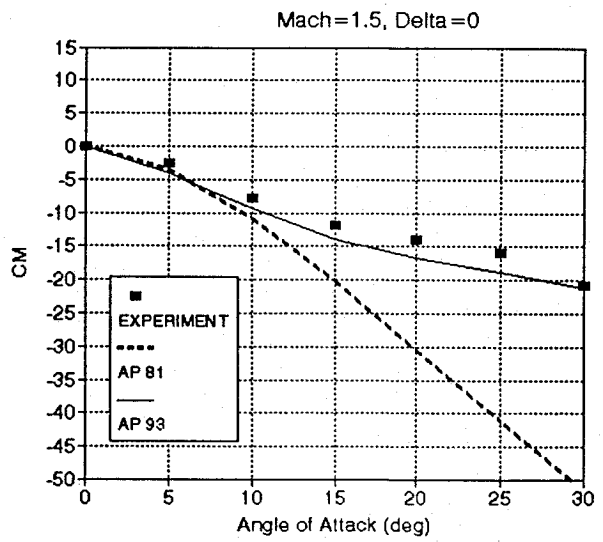

c) Pitching-moment coefficients at $M_\infty = 1.5$

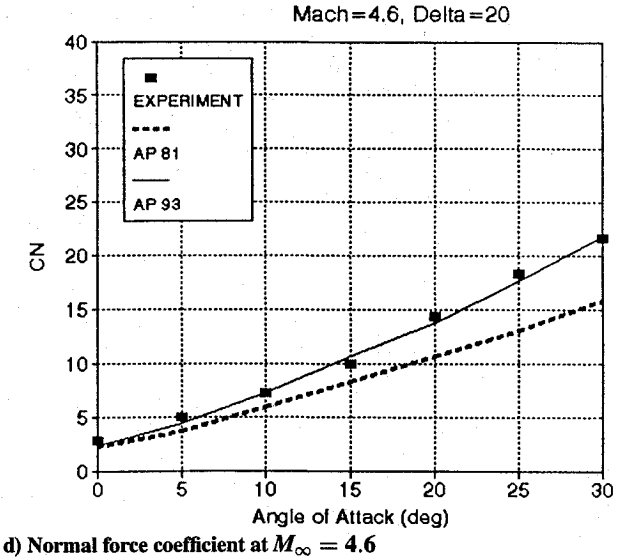

d) Normal force coefficient at $M_\infty = 4.6$

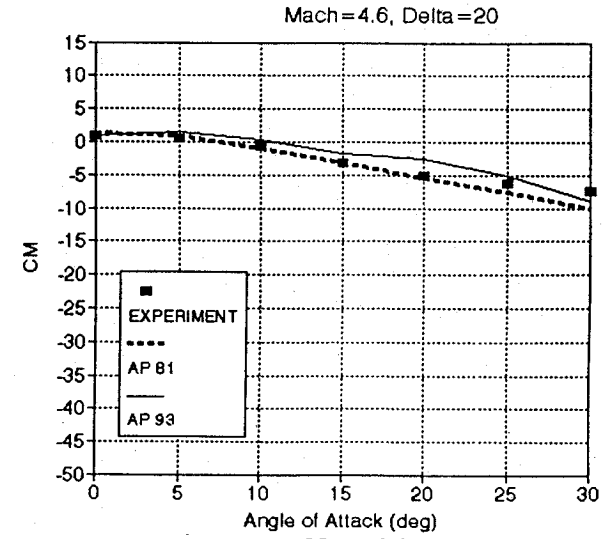

e) Pitching-moment coefficients at $M_\infty = 4.6$

Fig. 5 Air-to-air missile configuration[21,22] comparisons for $\delta = 0$.

two cases are presented. These are C_N and C_M at $M_\infty = 1.5$ and $\delta_W = 0$, and $M_\infty = 4.6$ and $\delta_W = 20$ deg (see Figs. 5b and 5c). For both conditions, the AP93 gives good agreement with experimental data and, for most conditions, gives significant improvements over the AP81 in comparison with the data. This configuration has fairly high-aspect-ratio wing and tail surfaces and is therefore an excellent example to illustrate the nonlinear capability of the AP93 code in comparison with the AP81 version.

A final configuration[26] for validation is another air-to-air missile, shown in Fig. 6a. This is a 100% blunt-nose case with aspect ratio-tails of 0.87 and canards of 1.7. Because the aspect ratio of the lifting surfaces is closer to 1 than those of Fig. 5, the AP81 code is expected to give better results compared to data than in the Fig. 5 case. This is true at most Mach numbers.[20] However, at low and high Mach numbers, the nonlinearities become more evident and the AP93 code gives significant improvement over the AP81. An example of this is shown for $M_\infty = 0.8$ and $\delta = 10$ deg in Fig. 6b. The AP93 shows improvement over the AP81 for C_N, C_A, and C_M at just about all conditions. However, as seen in Fig. 6b, the AP93 still predicts C_N too low at $M_\infty = 0.8$ and at higher values of α. It is not clear where this error comes from. Because the pitching-moment agreement is excellent, it is suspected that the canard and

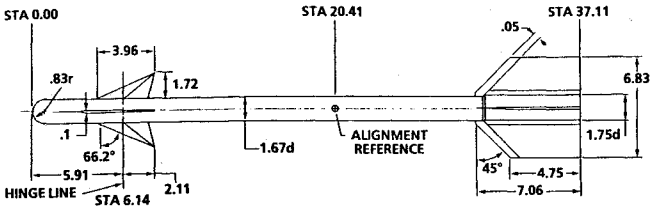

a) Geometry (dimensions in inches)

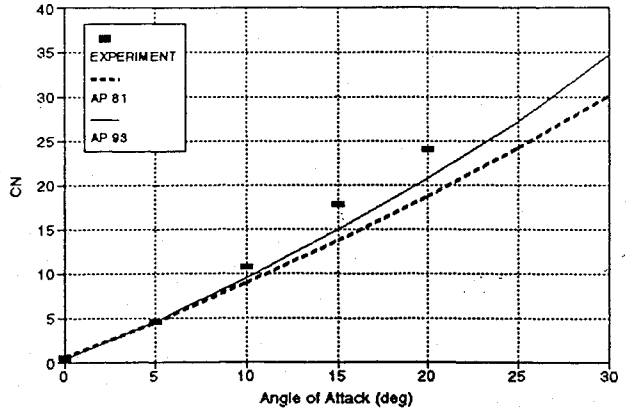

b) Normal-force coefficients

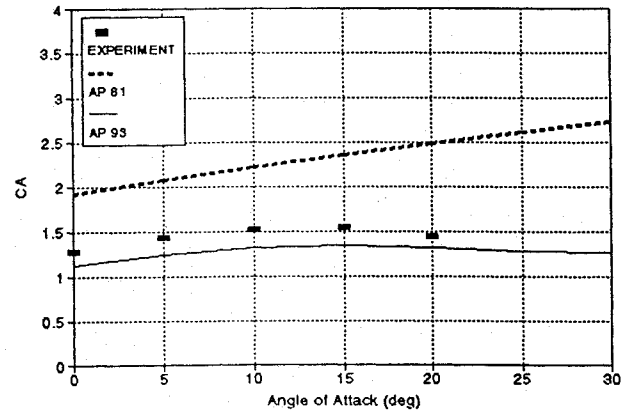

c) Axial-force coefficients

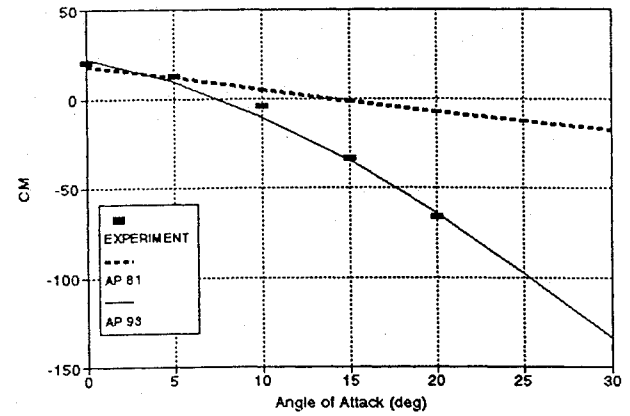

d) Pitching-moment coefficients

Fig. 6 Canard-body-tail configuration[26] comparisons for $M_\infty = 0.8$, $\delta = 10$ deg.

the tail are both underpredicted and by about the same amount. The body-alone normal force could also be slightly low.

Conclusions

In summary, an improved APC (AP93) has been developed. This paper summarizes the methodology for the new technology previously developed and documented, presents in more detail undocumented nonlinear methods for wing-body interference due to control deflection, and compares the new AP93 code with the previous APC (AP81) and experimental data.

New technology developed and included in the AP93 includes extension of the second-order shock-expansion theory to include real-gas effects; a new engineering method to calculate heat-transfer coefficients and adiabatic wall temperature; new approximate pressure prediction schemes for blunt and sharp bodies; an improved body-alone nonlinear lift prediction method; new nonlinear lift prediction methods for wing alone, wing-body interference, body-wing interference, and wing-body interference due to control deflection; and a new base-drag database to estimate the effects of AOA, fin location, and size, along with an improved empirical prediction model.

New capabilities of the code include the ability to calculate information to be used for conducting engineering estimates of heat transfer at high Mach numbers, the ability to use the code to get accurate estimates of nonlinear aerodynamics for low-aspect-ratio and low- or high-Mach-number aerodynamics up to AOAs of 30 deg, and improved axial-force estimations.

Comparison of the AP93 code with the AP81 version and experimental data showed that the AP93 code on average reduces the errors in normal-force and center-of-pressure estimation by one-half and gives slightly improved estimates of the axial-force coefficient.

The computational time of the AP93 is about the same as that of the AP81 version (less than 1 s per case on a CDC 995 computer). This is because many of the unused or seldom used techniques of the AP81 version were eliminated and replaced with more recent technology. There are a few new inputs, but these are minimal. In general, the AP93 has maintained the same ease of use (less than one-half day for an experienced user to set up a configuration for computational purposes) but is much more accurate and robust than the AP81 version. The code will be made available to legitimate requesting users at no charge to them.

Acknowledgments

Although the three coauthors were the principal personnel involved in the development of the AP93, other investigators have also contributed. These include Fred DeJarnette of North Carolina State University, Frank Baltakis of Advanced Technology Associates, Floyd Wilcox of the National Aeronautics and Space Administration/Langley Research Center, and Mike Armistead, Leroy Devan, and Steve Rowles from NSWCDD. Appreciation is expressed to each of these persons for their roles, which have been documented in previous technical reports. The work described in this report was supported through the Office of Naval Research (Dave Siegel) and, more specifically, the Surface-Launched Weapons Technology Block Program managed at NSWCDD by Robin Staton.

References

[1]Moore, F. G., "Body Alone Aerodynamics of Guided and Unguided Projectiles at Subsonic, Transonic, and Supersonic Mach Numbers," Naval Weapons Laboratory, TR-2796, Nov. 1972.

[2]Moore, F. G., "Aerodynamics of Guided and Unguided Weapons: Part I—Theory and Application," Naval Weapons Lab., TR-3018, Dec. 1973.

[3]Moore, F. G., and McKerley, W. C., "Aerodynamics of Guided and Unguided Weapons: Part II—Computer Program and Users Guide," Naval Weapons Lab., TR-3036, Jan. 1974.

[4]Moore, F. G., and Swanson, R. C., "Aerodynamics of Tactical Weapons to Mach Number 3 and Angle of Attack 15 Degrees: Part I—Theory and Application," NSWCDL, TR-3584, Feb. 1977.

[5]Swanson, R. C., and Moore, F. G., "Aerodynamics of Tactical Weapons to Mach Number 3 and Angle of Attack 15 Degrees: Part II—Computer Program and Usage," NSWCDL, TR-3600, March 1977.

[6]Devan, L., "Aerodynamics of Tactical Weapons to Mach Number 8 and Angle of Attack 180 °: Part I, Theory and Application," Naval Surface Warfare Center, TR 80-346, Oct. 1980.

[7]Devan, L., and Mason, L., "Aerodynamics of Tactical Weapons to Mach Number 8 and Angle of Attack 180 ° : Part II, Computer Program and Users Guide," Naval Surface Warfare Center,TR 81-358, Sept. 1981.

[8]Moore, F. G., Armistead, M., Rowles, S. H., and DeJarnette, F. R., "Second-Order Shock-Expansion Theory Extended to Include Real Gas Effects," Naval Surface Warfare Center, TR 90-683, Feb. 1992.

[9]Moore, F. G., Armistead, M., Rowles, S. H., and DeJarnette, F. R., "A New Approximate Method for Calculating Real Gas Effects on Missile Configurations," AIAA Paper 92-4637, Aug. 1992; also *Journal of Spacecraft*

and Rockets, Vol. 30, Jan.–Feb. 1993, pp. 22–31.

[10]McInville, R., and Moore, F., "Incorporation of Boundary Layer Heating Predictive Methodology into the NAVSWC Aeroprediction Code," Naval Surface Warfare Center, Dahlgren Division, TR-93/29, April 1993.

[11]Moore, F. G., Hymer, T., and Devan, L.,"New Methods for Predicting Nonlinear Lift, Center of Pressure, and Pitching Moment on Missile Configurations," Naval Surface Warfare Center, Dahlgren Division, TR-92/217, July 1992.

[12]Moore, F. G., Devan, L., and Hymer, T., "A New Semiempirical Method for Computing Nonlinear Angle-of-Attack Aerodynamics on Wing-Body-Tail Configurations," AIAA Paper, 93-0038; also *Journal of Spacecraft and Rockets*, Vol. 30, Nov.–Dec. 1993, pp. 696–706).

[13]Moore, F. G., Wilcox, F., and Hymer, T., "Improved Empirical Model for Base Drag Prediction on Missile Configurations Based on New Wind Tunnel Data," Naval Surface Warfare Center, Dahlgren Division, TR-92/509, Oct. 1992.

[14]Moore, F. G., Wilcox, F., and Hymer, T., "Base Drag Prediction on Missile Configurations," AIAA Paper 93-3629, Aug. 1993.

[15]Pitts, W. C., Nielsen, J. N., and Kaattari, G. E., "Lift and Center of Pressure of Wing-Body-Tail Combinations at Subsonic, Transonic, and Supersonic Speeds," NACA, TR 1307, 1957.

[16]Tsien, H. S., "Supersonic Flow over an Inclined Body of Revolution," *Journal of Aeronautical Sciences*, Vol. 5, No. 12, 1938.

[17]Klopfer, G. and Chausee, D., "Numerical Solution of Three-Dimensional Transonic Flows Around Axisymmetric Bodies at Angle of Attack," Nielsen Engineering and Research, Inc., TR-176, Feb. 1979.

[18]DeJarnette, F. R., Ford, C. P., and Young, D. E., "A New Method for Calculating Surface Pressures on Bodies at an Angle of Attack in Supersonic Flow," AIAA Paper 79-1552, July 1974.

[19]Allen, J. H., and Perkins, E. W., "Characteristics of Flow over Inclined Bodies of Revolution," NACA, RM A 50L07, March 1951.

[20]Moore, F. G., Hymer, T. C., and McInville, R. M., "Improved Aeroprediction Code: Part I—Summary of New Methods and Comparison with Experiment," Naval Surface Warfare Center, Dahlgren Division, TR-93/91, May 1993.

[21]McKinney, R. L., "Longitudinal Stability and Control Characteristics of an Air-to-Air Missile Configuration at Mach Numbers of 2.3 and 4.6 and Angles of Attack from −45° to 90°," NASA TM X-846, 1972.

[22]Monta, W. J., "Supersonic Aerodynamic Characteristics of a Sparrow III Type Missile Model with Wing Controls and Comparison with Existing Tail-Control Results," NASA TP 1078, Nov. 1977.

[23]Smith, E. H., Hebbar, S. K., and Platzer, M., "Aerodynamic Characteristics of a Canard-Controlled Missile at High Angles of Attack," AIAA Paper 93-0763, Jan. 1993.

[24]Trescott, C. D., and Foster, G. V., "Effect of Fin Planform on the Aerodynamic Characteristics of a Wingless Missile with Aft Cruciform Controls at Mach 1.6, 2.36, and 2.86," NASA TMX-2774, July 1973.

[25]Vukelich, S. R., Stoy, S. L., Burns, K. A., Castillo, J. A., and Moore, M. E., "Missile DATCOM Volume I—Final Report," Air Force Wright Aeronautical Lab., AFWALTR-86-3091, Wright Patterson AFB, OH, Dec. 1988.

[26]Graves, E., and Fournier, R., "Stability and Control Characteristics at Mach Numbers from 0.2 to 4.63 of a Cruciform Air-to-Air Missile with Triangular Canard Controls and a Trapezoidal Wing," NASA TM-X-3070, Nov. 1974.